Порядок с помощью вмороженного беспорядка во фрустрированном антиферромагнетике: эксперимент.

А.И.Смирнов

Институт физических проблем им. П. Л. Капицы РАН

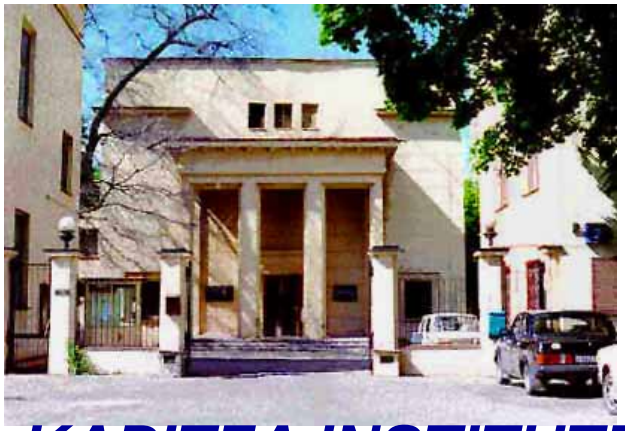

KAPITZA INSTITUTE

A.I. Smirnov, T. A. Soldatov ,

DE LA RECHERCHE À L'INDUSTRIE

cea

CEA Grenoble

M.Zhitomirsky

A.V.Shubnikov Institute of Crystallography

Russian Academy of Sciences

A. Ya. Shapiro

THE UNIVERSITY OF WARWICK

O.A. Petrenko

OSAKA UNIVERSITY

M. Hagiwara and his group

$$\hat{\mathcal{H}} = \sum_{\langle i,j \rangle} J_{ij} \hat{\mathbf{S}}_i \hat{\mathbf{S}}_j$$

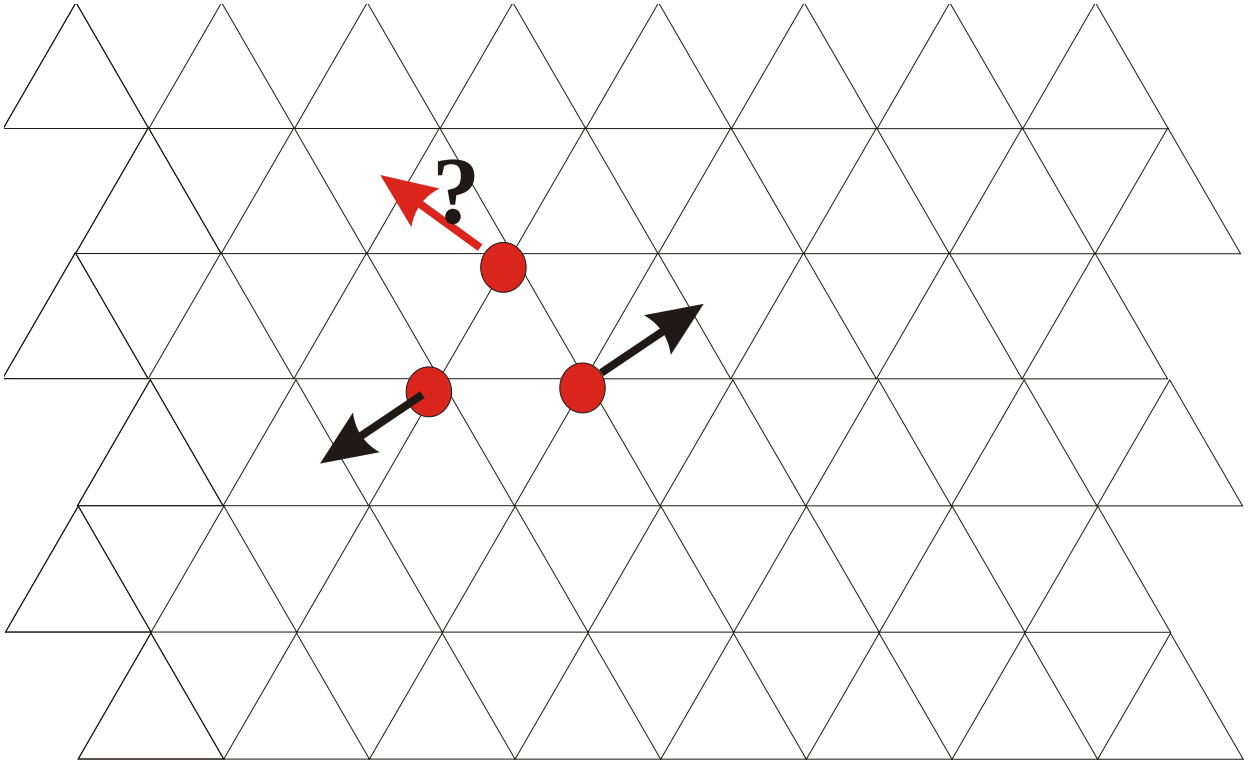

Frustration on a triangular lattice

Классическое основное состояние

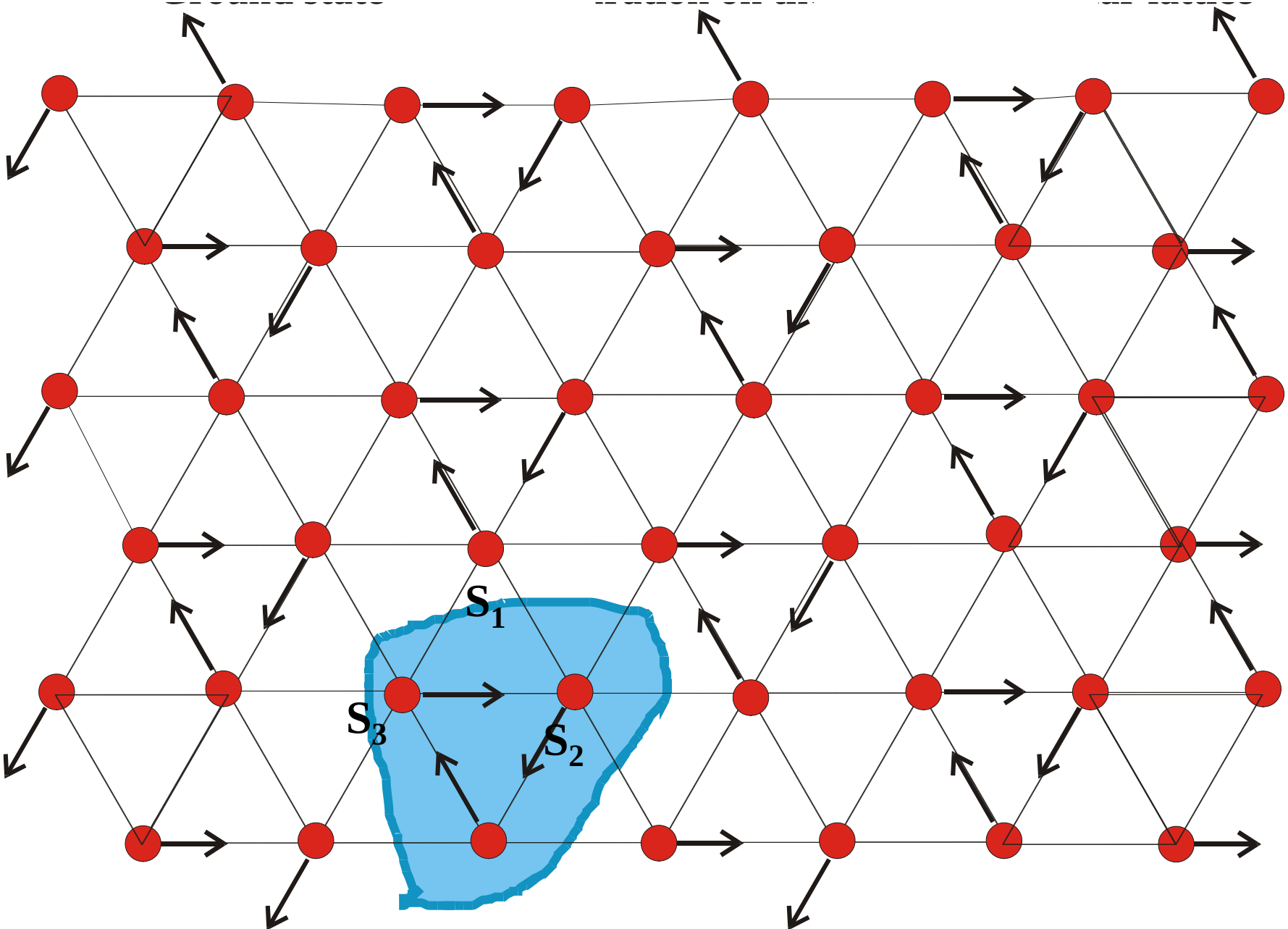

$$\hat{\mathcal{H}} = J\sum(\hat{S}_i\hat{S}_j)$$

Включим магнитное поле

$$\mathbf{M_1M_2} + \mathbf{M_1M_3} + \mathbf{M_2M_3} = \frac{1}{2}[(M_1 + M_2 + M_3)^2 - M_1^2 - M_2^2 - M_3^2]$$

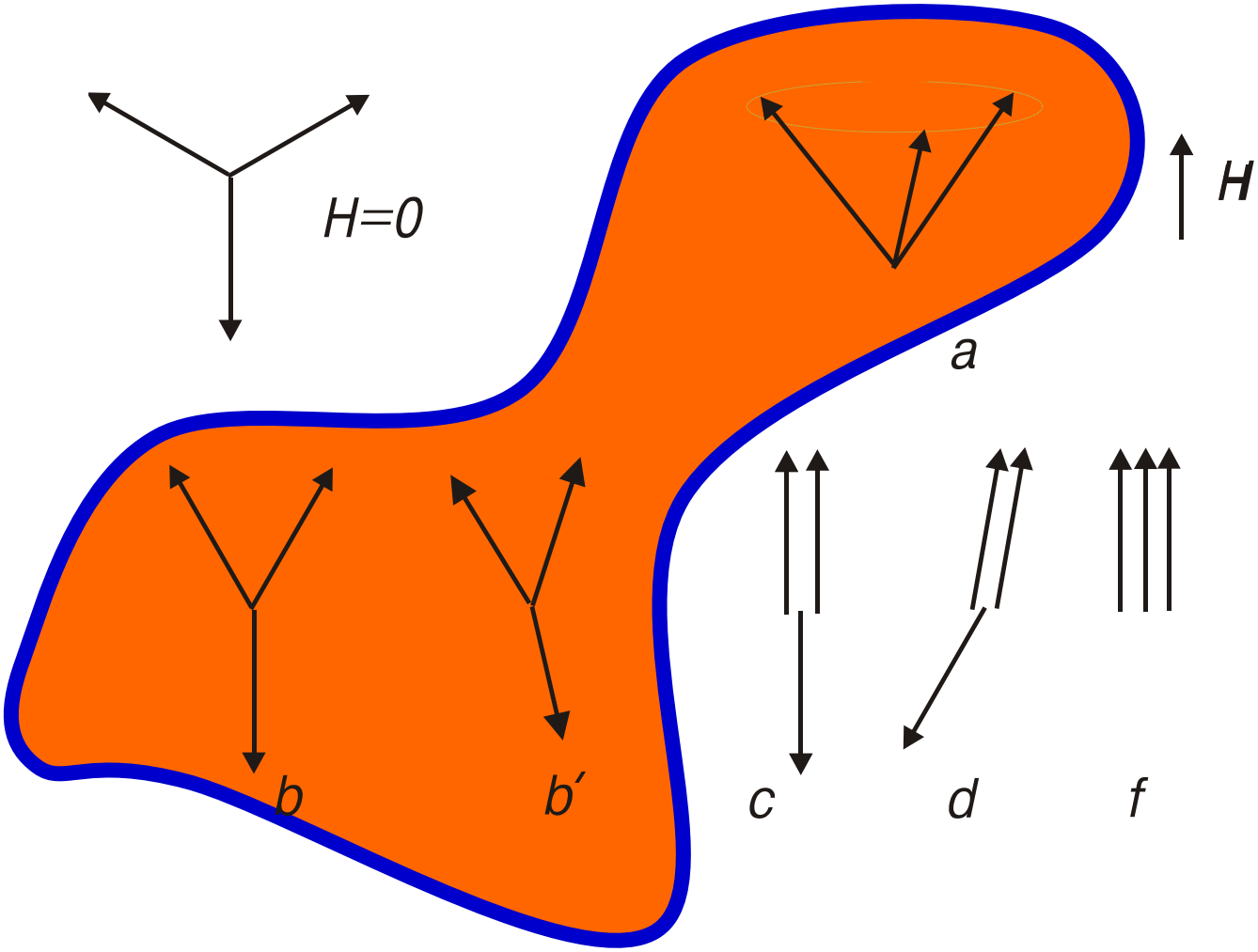

В магнитном поле все состояния с одинаковой суммой $\boldsymbol{M}_1+\boldsymbol{M}_2+\boldsymbol{M}_3$ вырождены

Отбор основного состояния с учетом флуктуаций ("порядок через беспорядок")

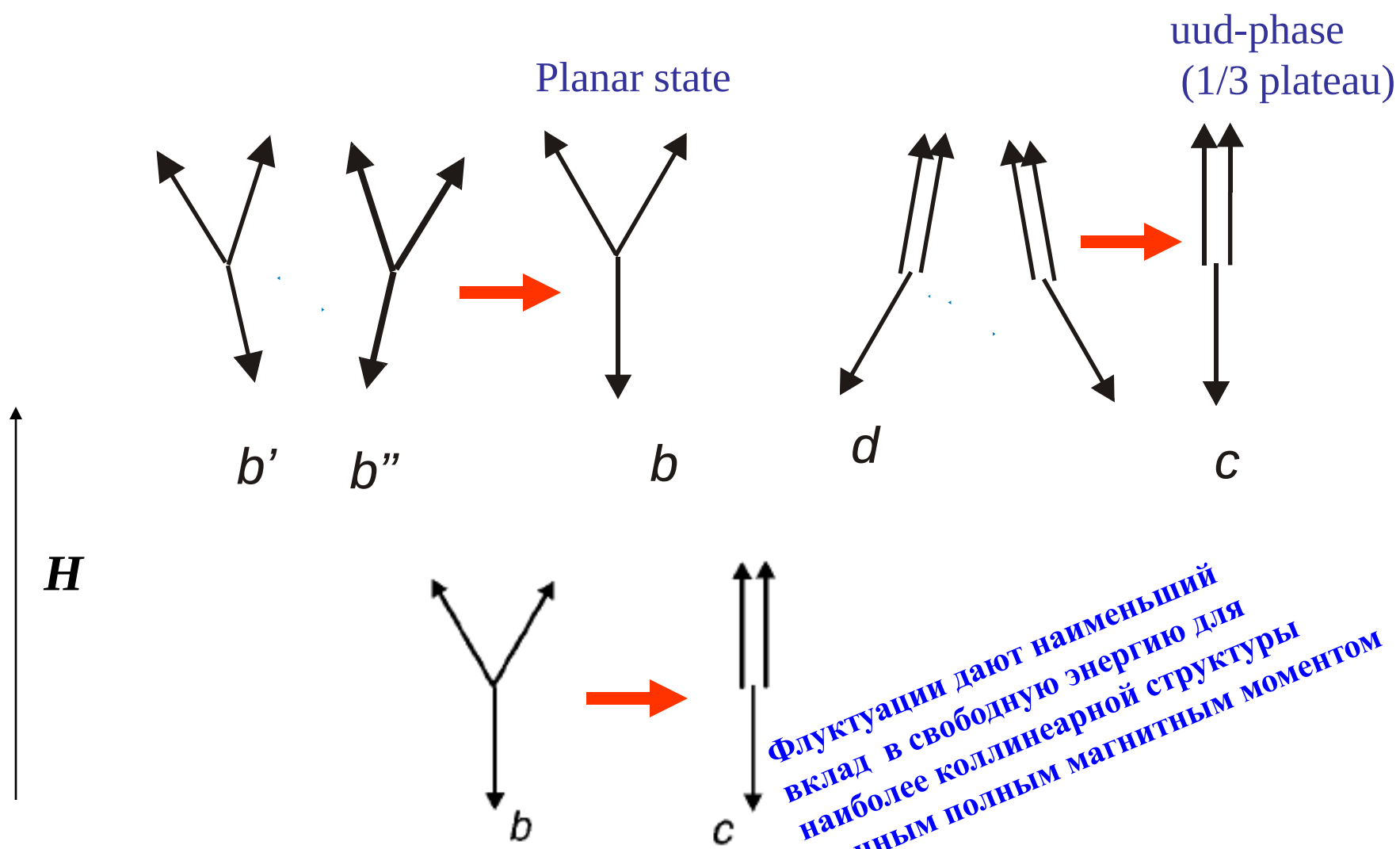

Флуктуации дают наименьший вклад в свободную энергию для наиболее коллинеарной структуры данным полным магнитным моментом

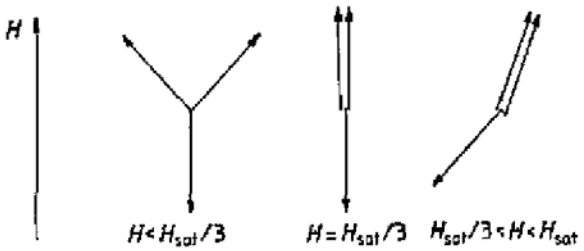

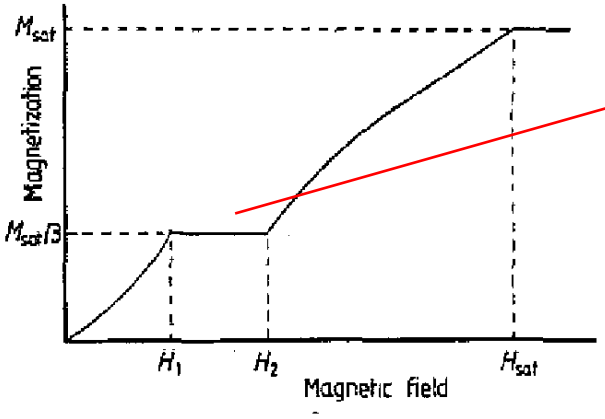

Figure 3. The anticipated behaviour of longitudinal magnetization in 2D Heisenberg AFM on a triangular lattice. The plateau on the magnetization curve results from the stabilization of the collinear phase in the finite region of magnetic fields due to zero-point motion.

Kawamura &Miyashita JPSJ 54 1985

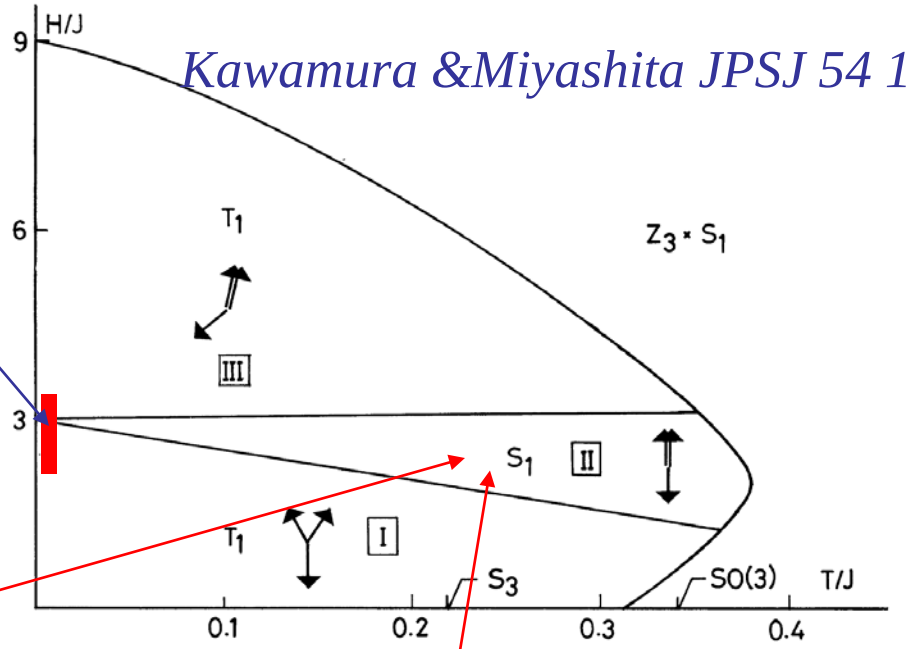

5. Temperature-magnetic field phase diagram of the AFT Heisenberg model. The effective symmetry and the stable spin configurations are also shown for each phase. Note that the location of phase boundaries may not be very precise.

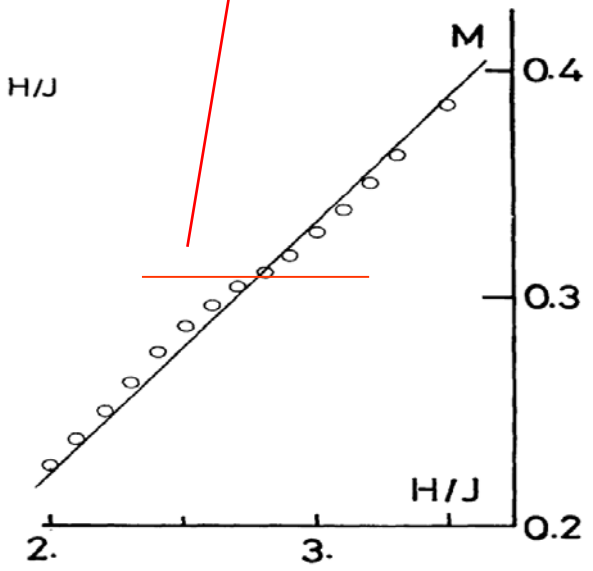

Heisenberg model including fluctuations

Модельный треугольный антиферромагнетик $RbFe(MoO_4)_2$

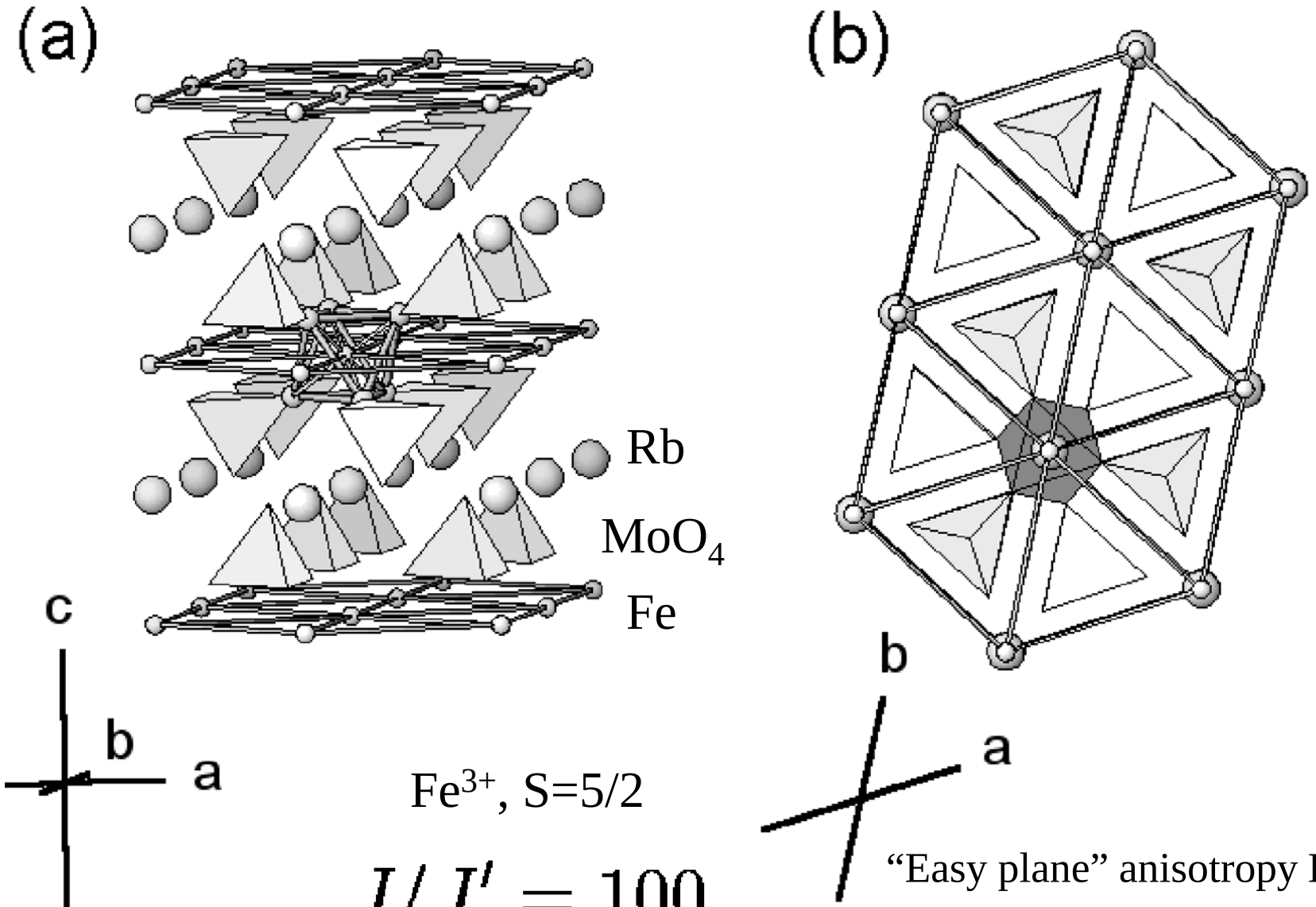

Fe^{3+}, S=5/2

$$J/J' = 100$$

“Easy plane” anisotropy D~J/2

1/3 plateau confirmed in RbFe(MoO4)2

Static field

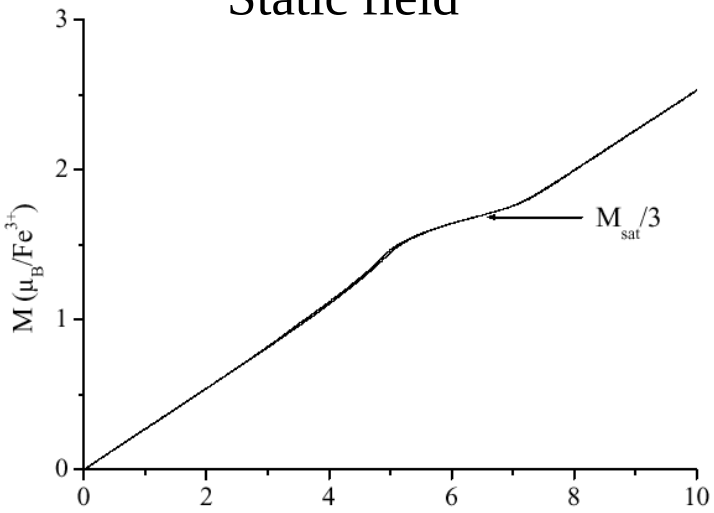

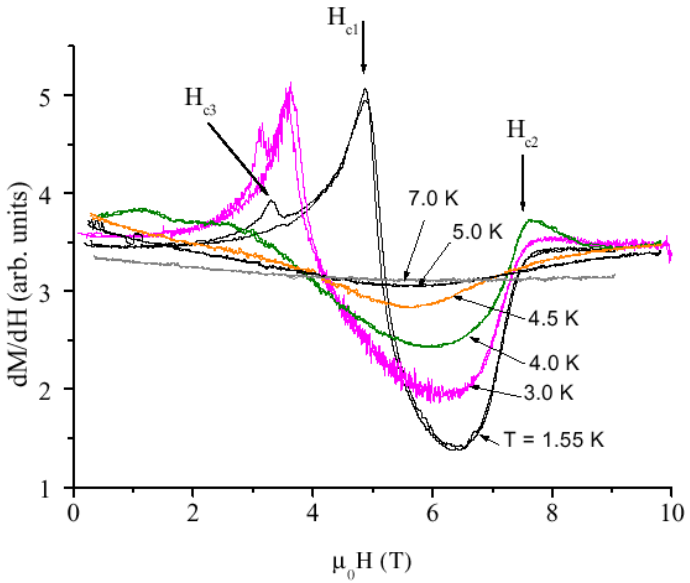

Svistov et al PRB 2006

Pulse field

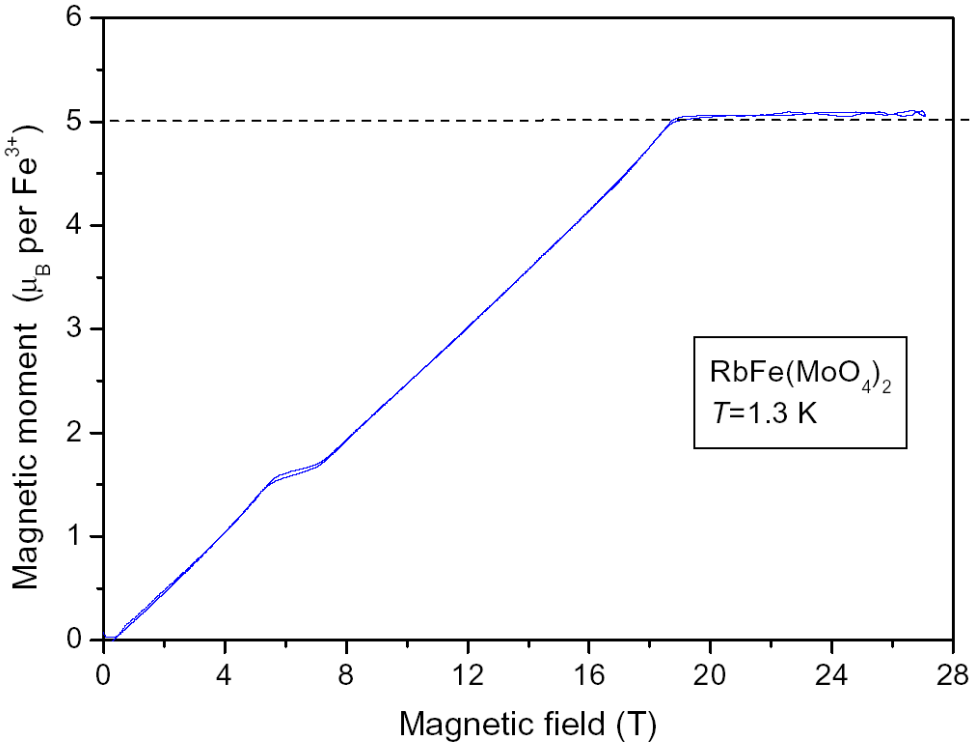

Smirnov et al PRB 2007

Comparison of theory (2D TAFM of XY & Heisenberg type)
and experiment ($RbFe(MoO_4)_2$, S=5/2, easy-plane anisotropy with D~J/2)

J=1.2 K from susceptibility

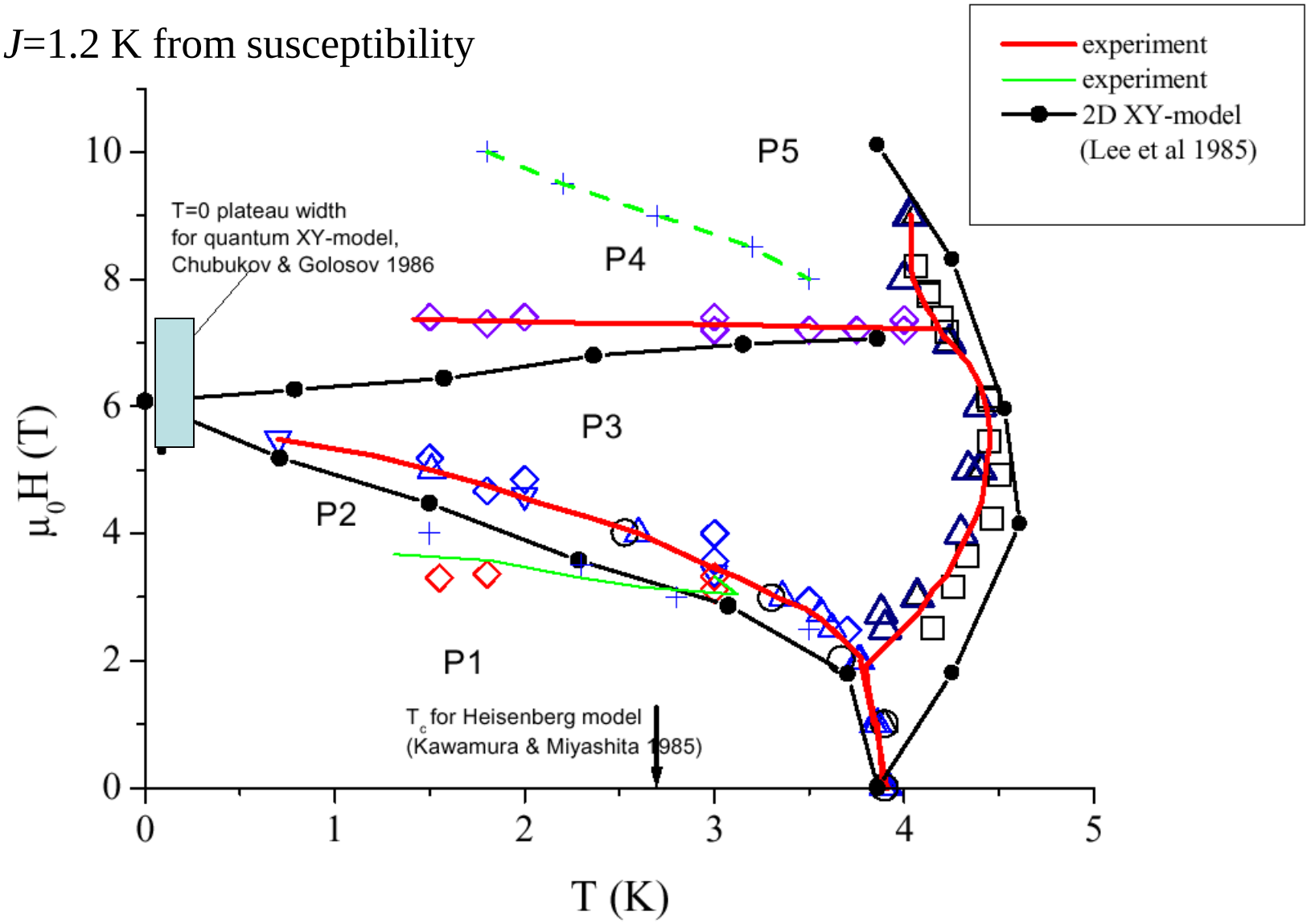

Svistov et al PRB 2006

Нейтронные исследования RbFe(MoO4)2

PRL **98,** 267205 (2007) PHYSICAL REVIEW LETTERS week ending 29 JUNE 2007

Direct Transition from a Disordered to a Multiferroic Phase on a Triangular Lattice

M. Kenzelmann,[1,2,3] G. Lawes,[4,5] A. B. Harris,[6] G. Gasparovic,[2,3] C. Broholm,[2,3] A. P. Ramirez,[4,7] G. A. Jorge,[8] M. Jaime,[8] S. Park,[3,9] Q. Huang,[3] A. Ya. Shapiro,[10] and L. A. Demianets[10]

[1]*Laboratory for Solid State Physics, ETH Zurich, CH-8093 Zurich, Switzerland*
[2]*Department of Physics and Astronomy, The Johns Hopkins University, Baltimore, Maryland 21218, USA*
[3]*NIST Center for Neutron Research, National Institute of Standards and Technology, Gaithersburg, Maryland 20899, USA*

PHYSICAL REVIEW B **88**, 060409(R) (2013)

Multiferroicity in the generic easy-plane triangular lattice antiferromagnet $RbFe(MoO_4)_2$

J. S. White,[1,2] Ch. Niedermayer,[1] G. Gasparovic,[3,4] C. Broholm,[3,4] J. M. S. Park,[5] A. Ya. Shapiro,[6] L. A. Demianets,[6] and M. Kenzelmann[7]

[1]*Laboratory for Neutron Scattering, Paul Scherrer Institut, CH-5232 Villigen, Switzerland*
[2]*Laboratory for Quantum Magnetism, Ecole Polytechnique Fédérale de Lausanne, CH-1015 Lausanne, Switzerland*
[3]*Institute for Quantum Matter and Department of Physics and Astronomy, The Johns Hopkins University, Baltimore, Maryland 21218, USA*
[4]*NIST Center for Neutron Research, National Institute of Standards and Technology, Gaithersburg, Maryland 20899, USA*
[5]*Neutron Science Division, Korea Atomic Energy Research Institute, Daejeon 305-353, Republic of Korea*
[6]*A. V. Shubnikov Institute for Crystallography RAS, 117333 Moscow, Russia*
[7]*Laboratory for Developments and Methods, Paul Scherrer Institut, CH-5232 Villigen, Switzerland*
(Received 29 March 2013; published 27 August 2013)

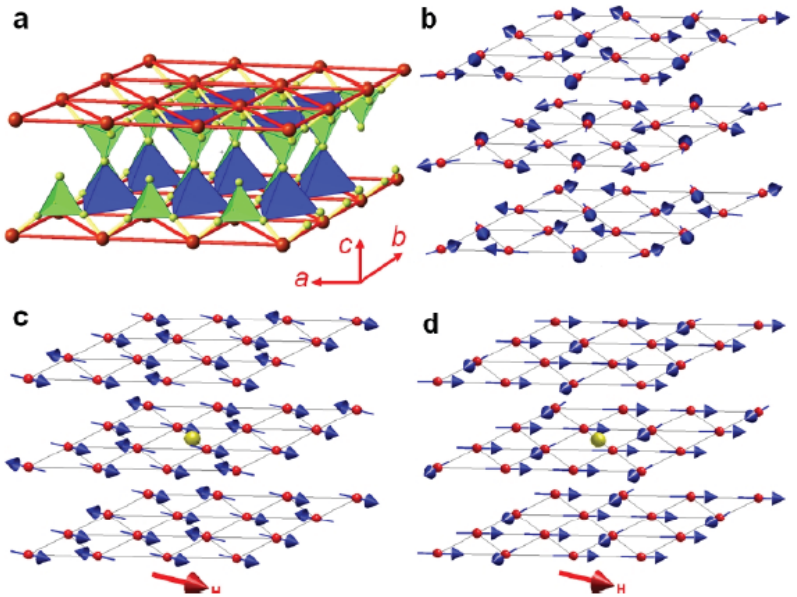

FIG. 1 (color). (a) Low-temperature chemical structure of RFMO, belonging to the trigonal space group $P\bar{3}$. Shown are the Fe^{3+} in red and O^{-2} ions in yellow. The Fe^{3+} are expected to interact through superexchange involving two O^{-2} for intraplane interactions and three O^{-2} for interplane interactions. There is one nearest-neighbor and two distinct next-nearest-neighbor interactions between planes. (b) Zero-field magnetic structure at $T = 2$ K with an ordered moment at each site $M = 3.9(5)\mu_B$; (c) at $\mu_0 H = 6$ T and $T = 2$ K, two-thirds of the moments point with $M = 3.8(3)\mu_B$ along the field direction and one-third with $M = 2.8(3)\mu_B$ opposite to it; and (d) at $\mu_0 H = 10$ T and $T = 0.1$ K, with $M = 3.7(5)\mu_B$, one-third of the moments are perpendicular to the field and two-thirds are parallel to each other and form an angle of 30° with the field direction. The structures shown in (c),(d) have an inversion center indicated by the yellow point.

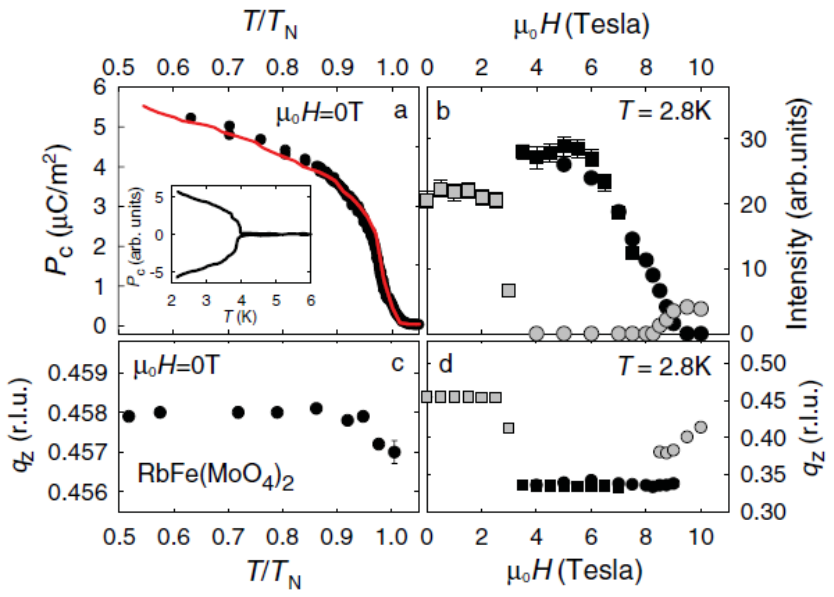

FIG. 2 (color). (a) Zero-field temperature dependence of the magnetic Bragg intensity (solid circles) observed at $\mathbf{Q} = (1/3, 1/3, q_z)$ compared to that of the ferroelectric polarization (solid line) P_c along the c axis. Inset: P_c measured under positive and negative poling biases. (b) Field dependence of the intensity at $T = 2.8$ K for the commensurate (black) and the incommensurate (gray) reflections. The commensurate and the high-field incommensurate orders coexist at this temperature for a narrow field region between $\mu_0 H = 8$ and 9 T. (c),(d) Temperature and field dependence of q_z at zero field and at $T = 2.8$ K, respectively. Squares and circles in (b),(d) distinguish two independent measurements, for which intensities were put on the same scale by matching data measured at the same field.

In-plane magnetic fields applied along the $[1, -1, 0]$

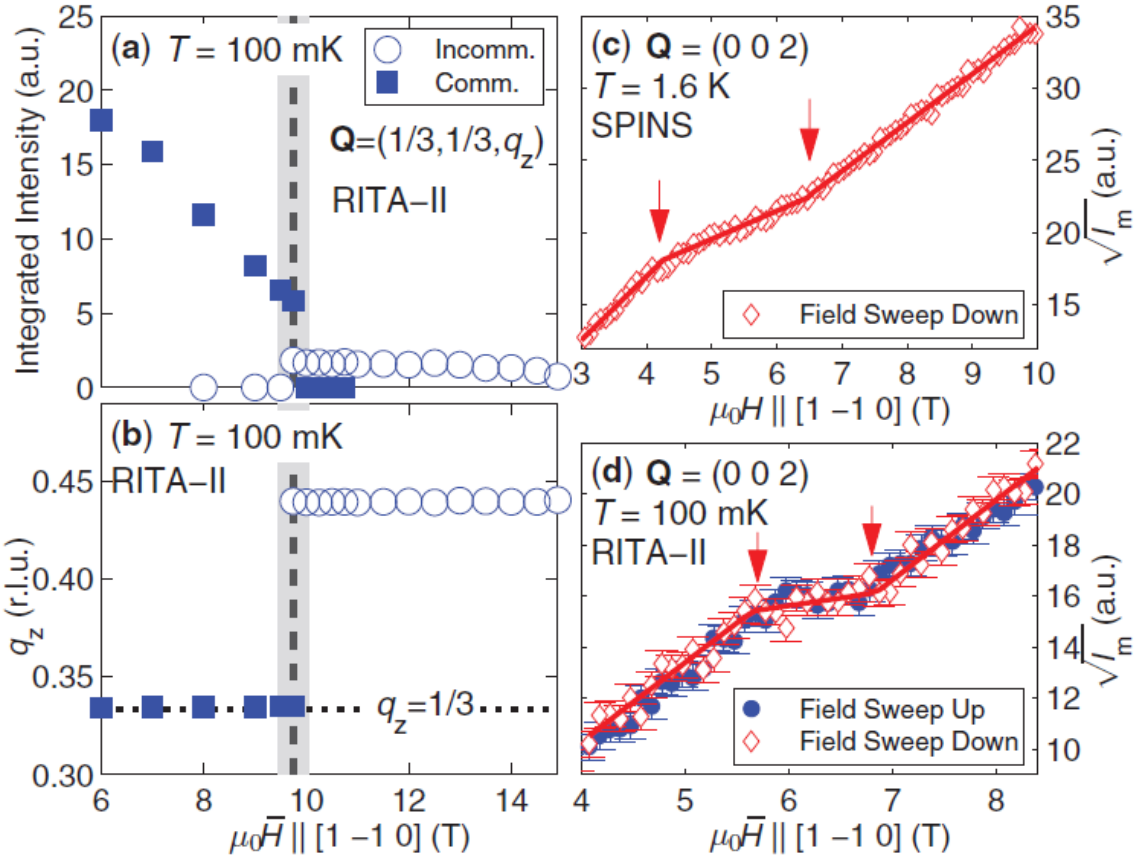

FIG. 3. (Color online) The $\mu_0 H$ dependence at $T = 100$ mK of (a) the neutron integrated intensity recorded at the $Q = (1/3, 1/3, q_z)$ position, and (b) the q_z component. Dashed lines mark the transition fields between different phases, with the uncertainties indicated by the shaded regions. At (c) $T = 1.6$ K and (d) $T = 100$ mK we show the $\mu_0 H$ dependence of the square root of the magnetic neutron intensity $\sqrt{I_m}$ measured at the (002) position. Red arrows indicate the field range of the intensity plateaus.

Треугольный антиферромагнетик с немагнитными примесями: конкуренция флуктуаций и вмороженного беспорядка

PRL 111, 247201 (2013) PHYSICAL REVIEW LETTERS week ending 13 DECEMBER 2013

Triangular Antiferromagnet with Nonmagnetic Impurities

V. S. Maryasin and M. E. Zhitomirsky
Service de Physique Statistique, Magnétisme et Supraconductivité, UMR-E9001 CEA-INAC/UJF, 17 rue des Martyrs, 38054 Grenoble, France
(Received 26 September 2013; revised manuscript received 19 November 2013; published 9 December 2013)

The effect of nonmagnetic impurities on the phase diagram of the classical Heisenberg antiferromagnet on a triangular lattice is investigated. We present analytical arguments confirmed by numerical calculations that at zero temperature vacancies stabilize a conical state providing an example of "order by quenched disorder" effect. Competition between thermal fluctuations and the site disorder leads to a complicated H–T phase diagram, which is deduced from the classical Monte Carlo simulations for a representative vacancy concentration. For the XY triangular-lattice antiferromagnet with an in-plane external field, nonmagnetic impurities stabilize the fanlike spin structure. We also briefly discuss the effect of quantum fluctuations.

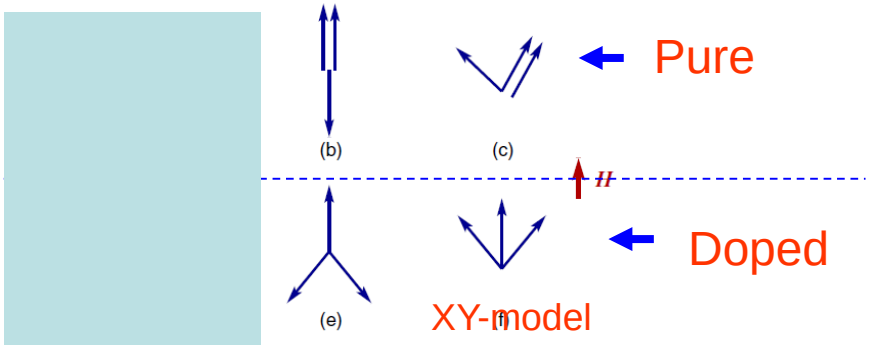

FIG. 1 (color online). Ordered magnetic states of a TAFM in an external field. Spin configurations appearing for the TAFM without impurities: (a) coplanar Y state, (b) collinear uud state, and (c) coplanar 2:1 (V) state. Spin configurations in the presence of nonmagnetic impurities: (d) conical (umbrella) state of the Heisenberg TAFM, (e) anti-Y state and equivalent (f) fan state of the XY TAFM.

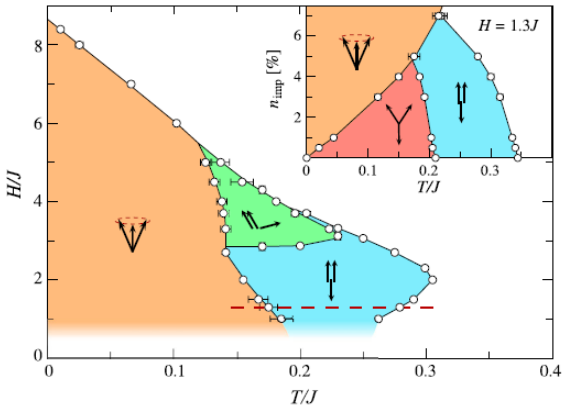

FIG. 3 (color online). Classical Monte Carlo phase diagram of the Heisenberg TAFM with 5% of nonmagnetic impurities. Solid lines via data points are guides for the eye. The inset shows the concentration evolution of ordered phases for $H/J = 1.3$, which is indicated by the dashed line on the main panel.

Correlation of short-period oscillatory exchange coupling to nanometer-scale lateral interface structure in Fe/Cr/Fe(001)

C. M. Schmidt, D. E. Bürgler,* D. M. Schaller, F. Meisinger, and H.-J. Güntherodt
Institut für Physik, Universität Basel, Klingelbergstrasse 82, CH-4056 Basel, Switzerland

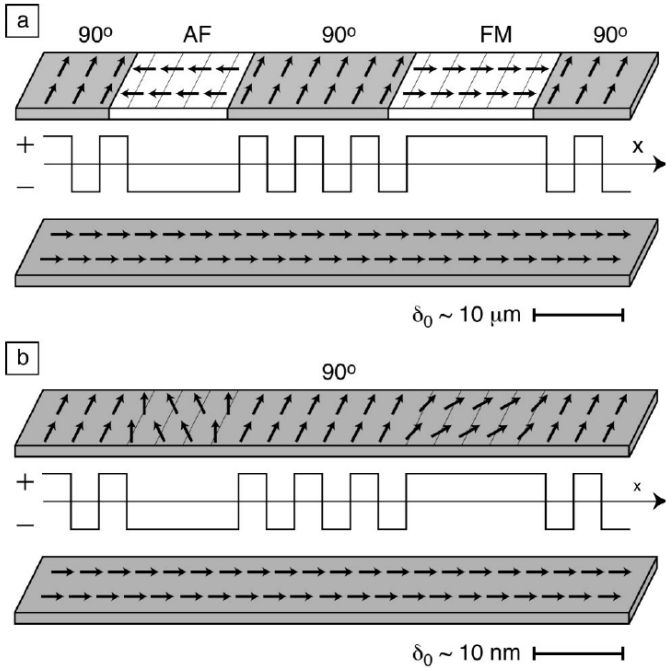

FIG. 12. Schematic response of the top Fe layer to the H_{ex} profile shown between the Fe layers under the assumption of a homogeneously magnetized bottom Fe layer. (a) For δ_0 of the order of micrometers, FM and AF domains develop at the positions of pillars, and 90° domains in between. (b) For δ_0 of the order of nanometers, the spin orientation of the top Fe layer is locally perturbed, resulting in positive or negative angular deviations from the overall 90° coupling. All magnetizations are in-plane.

Static disorder affects magnetic order.

Статический беспорядок препятствует флуктуационному механизму “порядок через беспорядок” отбора основного состояния из множества вырожденных состояний. Формально биквадратичный обмен $T(\boldsymbol{S}_i\boldsymbol{S}_j)^2$ отрицателен для чистых и положителен для допированных образцов.

Чистый образец: в слабом поле выгодна наиболее коллинеарная структура (Y-типа)
Образец с примесями: предпочтительна наиболее неколлинеарная структура (анти-Y).

В нашем эксперименте мы проверяем эти предсказания.

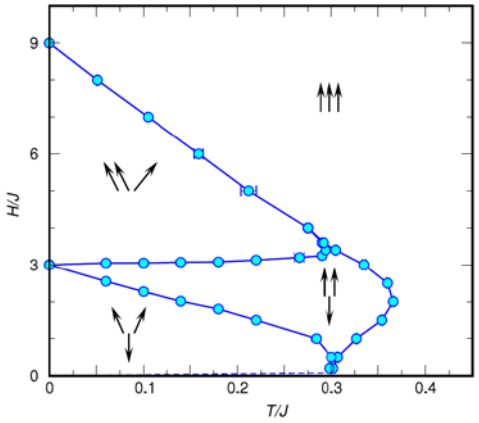

Figure 3. Magnetic field phase diagram of the Heisenberg triangular-lattice antiferromagnet. Transition points determined by the Monte Carlo simulations are shown by circles. Solid lines are guides for the eye. Dashed line indicates the position of additional low-field transitions.

Немагнитное допирование

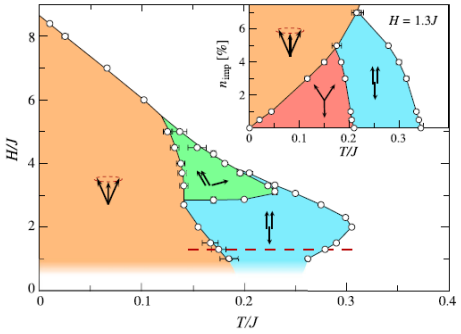

FIG. 3 (color online). Classical Monte Carlo phase diagram of the Heisenberg TAFM with 5% of nonmagnetic impurities. Solid lines via data points are guides for the eye. The inset shows the concentration evolution of ordered phases for $H/J = 1.3$, which is indicated by the dashed line on the main panel.

Хаотическая модуляция обменных связей производится путем замещения Rb на K

$Rb_{1-x}K_xFe(MoO_4)_2$, (x=0, 0.025, 0.05, 0.075, 0.15,)

Восприимчивость образцов $Rb_{1-x}K_xFe(MoO_4)_2$ с различной концентрацией калия

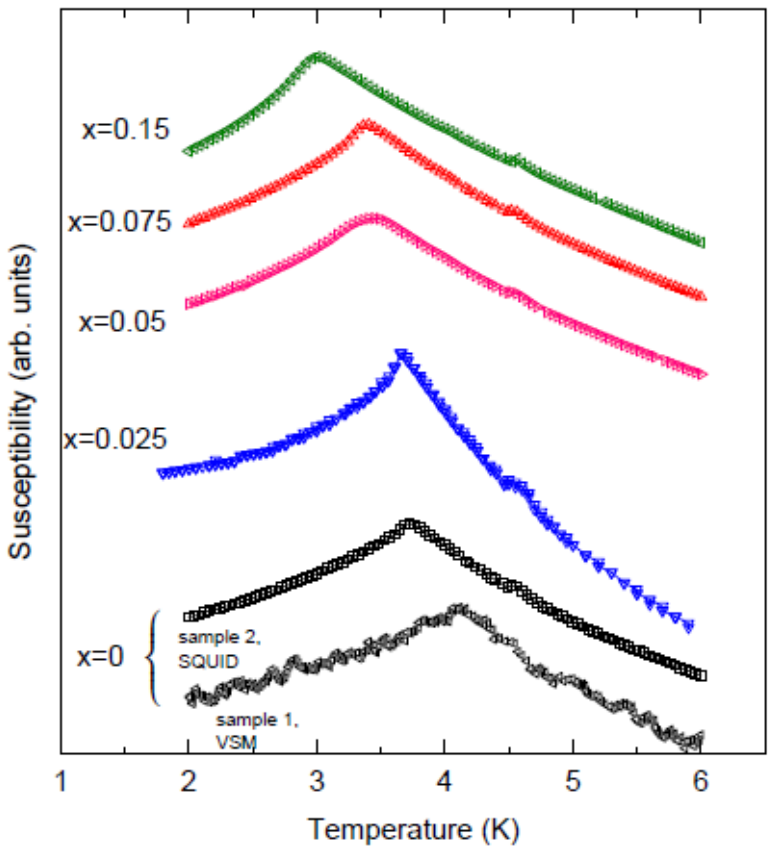

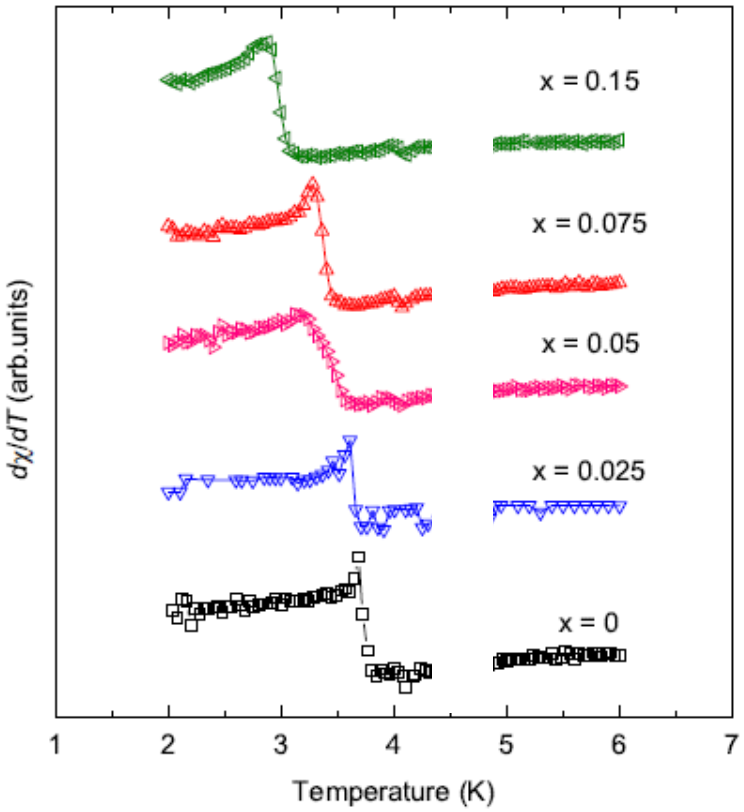

Допирование калием приводит к небольшому сдвигу T_N без существенного размытия перехода

Smirnov et al PRL 2017

Кривые намагничивания: плато “1/3” исчезает в образцах с примесями, но частично восстанавливается при нагревании

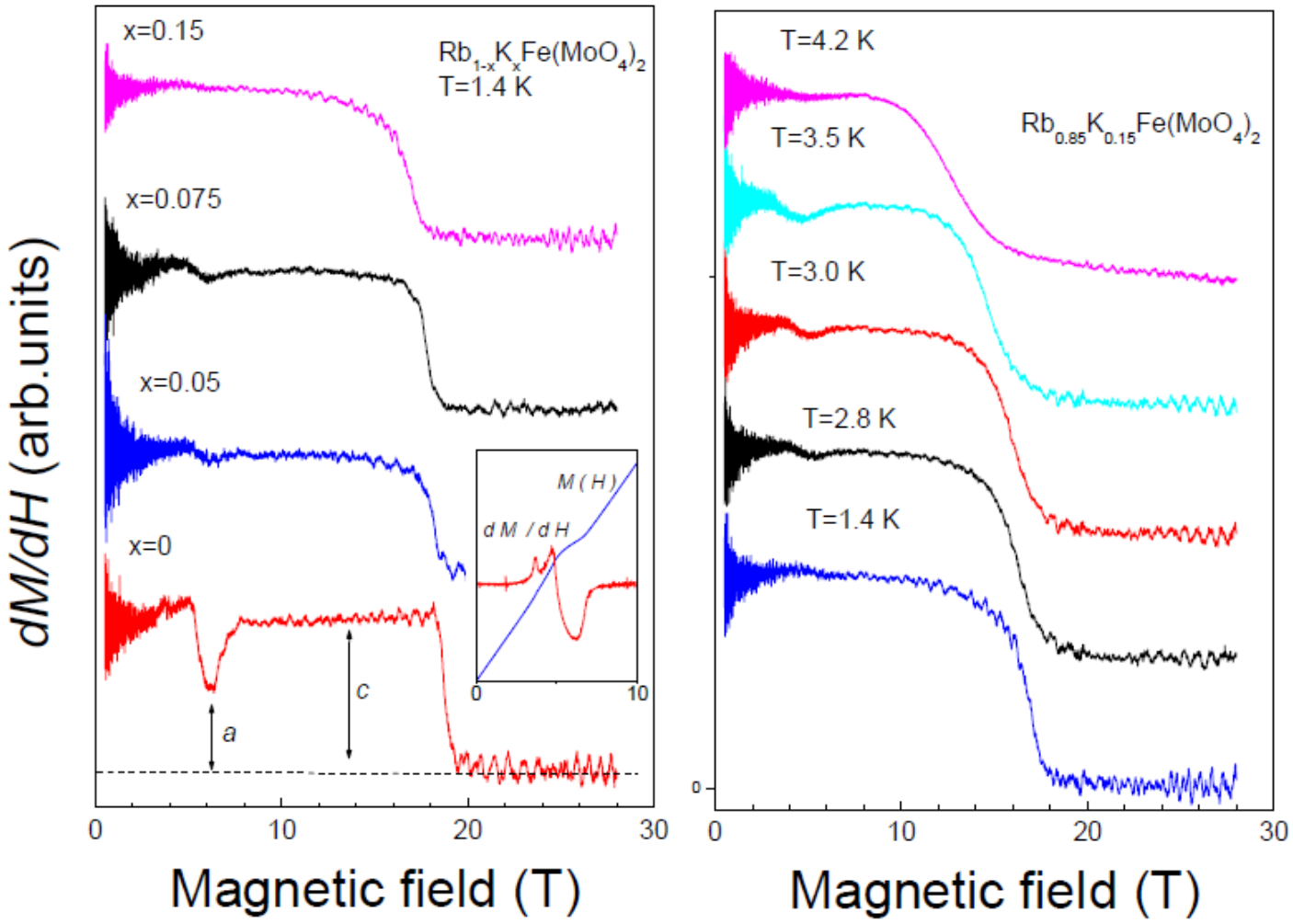

Q=1-a/c

Smirnov et al PRL 2017

Q - качество плато: Q=1-a/c; Q=1 для идеального горизонтального плато,
Q=0 для отсутствия аномалии

Δ – щель в спектре АФМР
T_N – температура Нееля
H_{sat} – поле насыщения.

Зависимость качества плато и параметров T_N, Δ , H_{sat} от концентрации калия

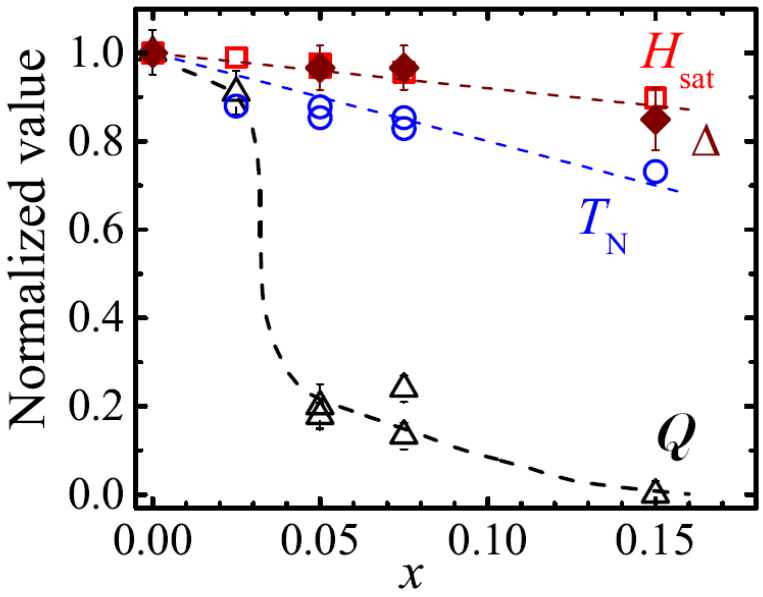

Температурная зависимость качества плато в разных образцах $Rb_{1-x}K_xFe(MoO_4)_2$

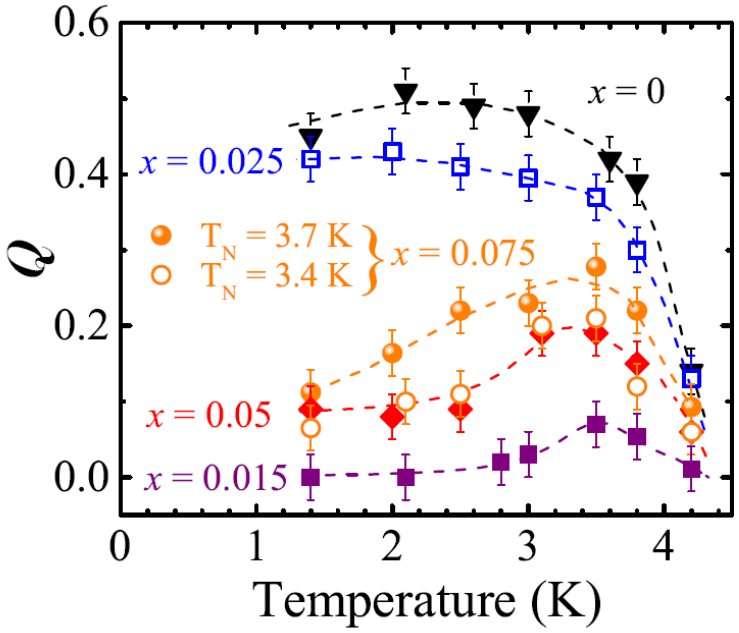

ESR spectrum of ***pure*** $RbFe(MoO_4)_2$, in-plane magnetic field

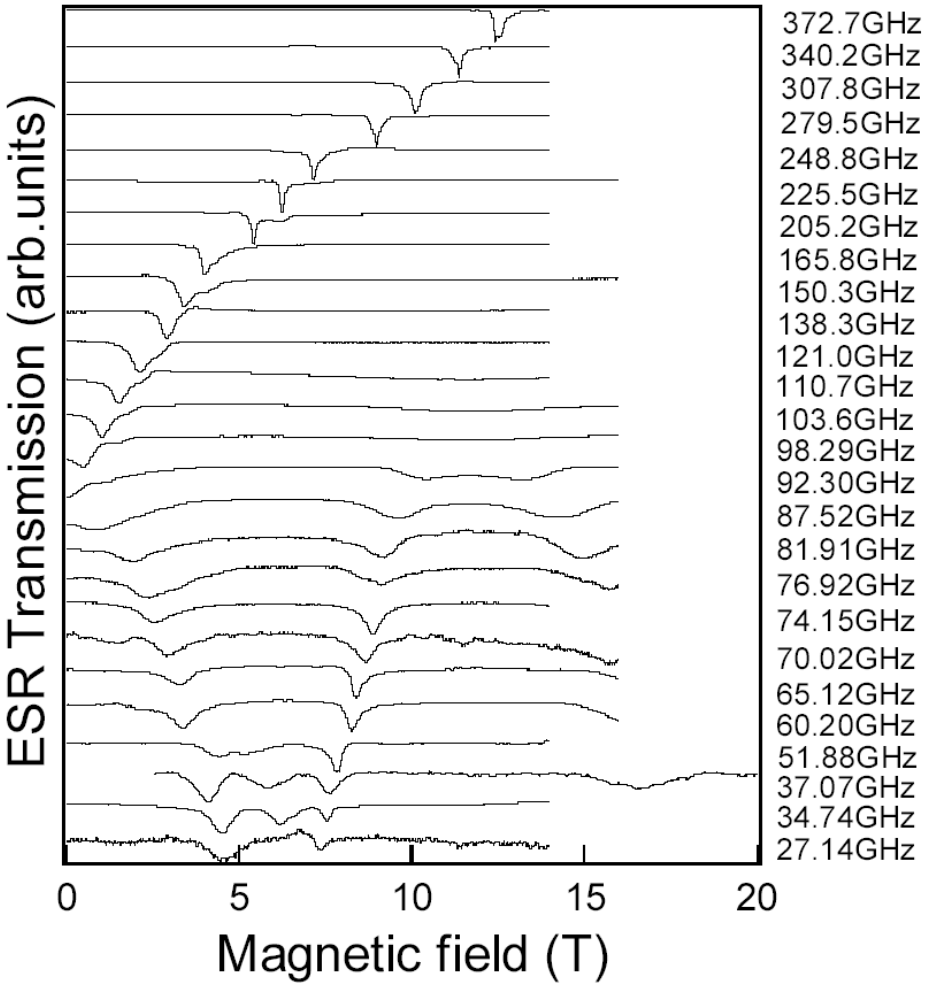

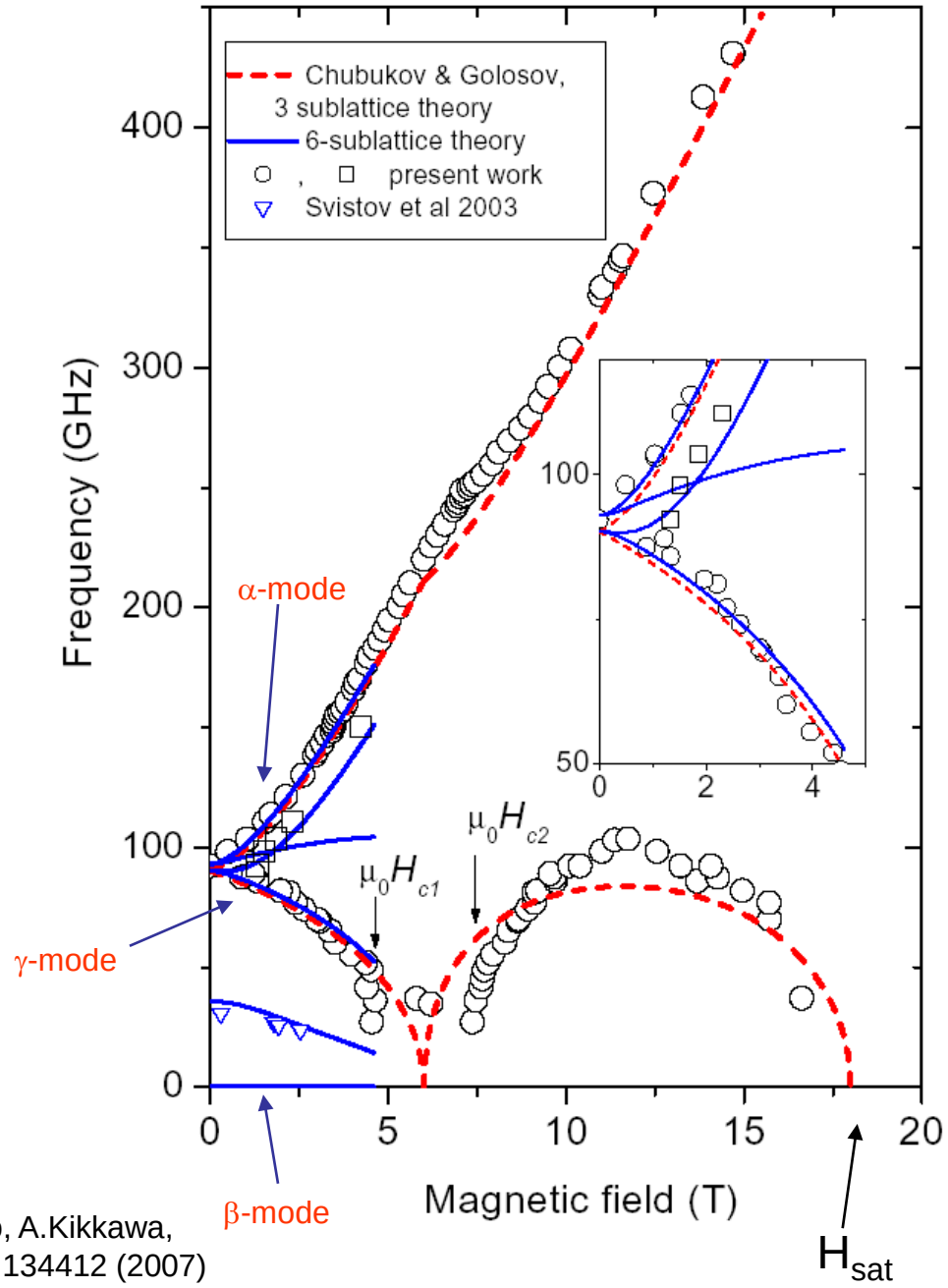

A.I.Smirnov, H.Yashiro, S.Kimura, M.Hagiwara, Y.Narumi, K.Kindo, A.Kikkawa, K.Katsumata, A.Ya.Shapiro, and L.N.Demianets, Phys. Rev B 75, 134412 (2007)

ЭСР- спектры для чистого и допированного образцов

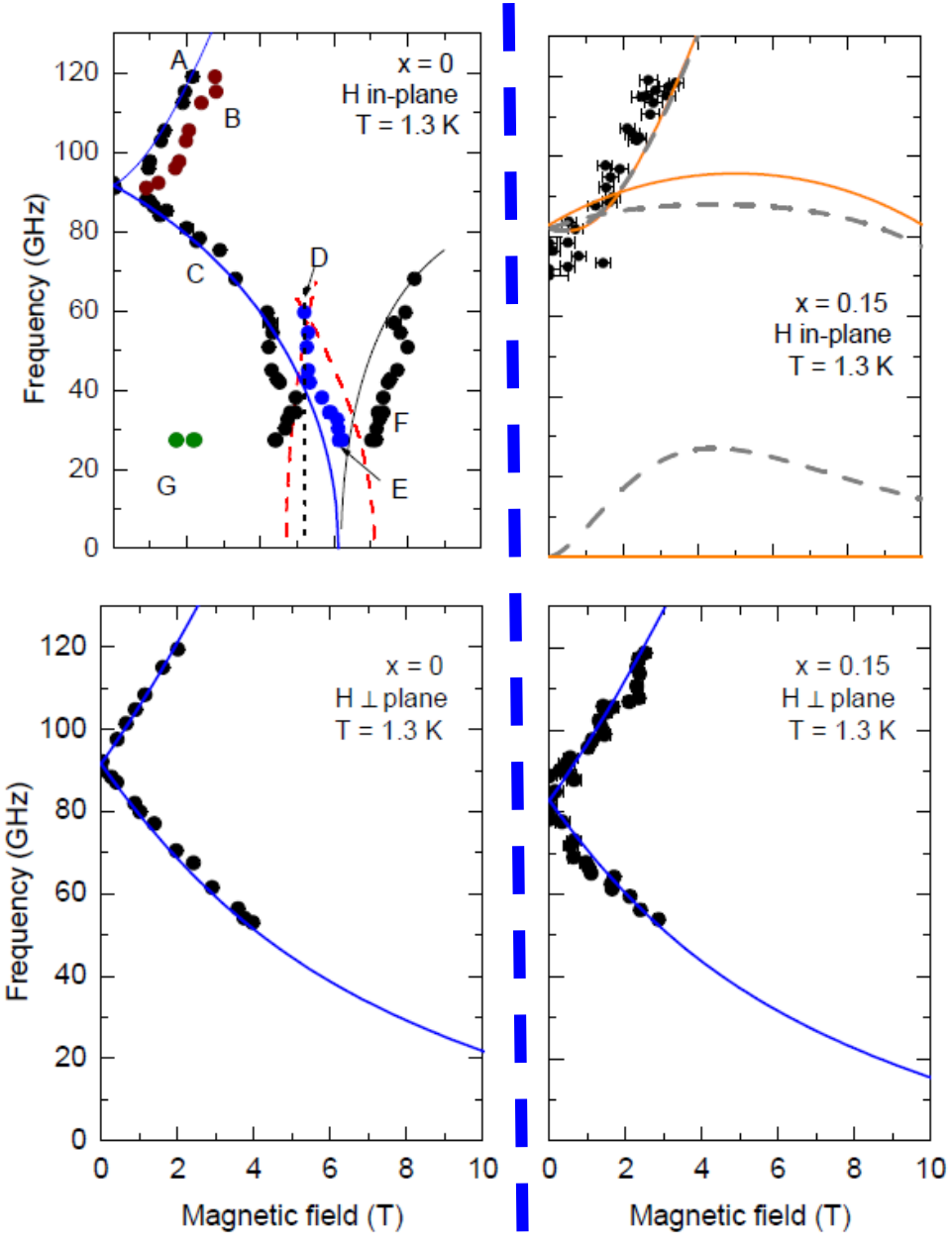

Smirnov et al PRL 2017

Теория для Y-структуры

Теория для анти-Y структуры
пунктир – с учетом положи-
тельного биквадратичного
обмена

$$\omega_1 = 3JS\sqrt{d(1\mp h)(3\pm h)}\ , \quad d = \frac{D}{3J}$$

$$\omega_2 = 3JS\sqrt{2d + h^2 + d(1\pm h)^2}\ , \quad h = \frac{g\mu_B H}{3JS}$$

Теория для зонтичной
структуры

$$\omega_1 = \frac{9}{2}JS\left[\sqrt{\sin^2\alpha + (4D/9J)\cos^2\alpha} + \sin\alpha\right]$$

$$\omega_2 = \frac{9}{2}JS\left[\sqrt{\sin^2\alpha + (4D/9J)\cos^2\alpha} - \sin\alpha\right]$$

$$\sin\alpha = H/H_s$$

Переход
“Y”- “анти - Y”
при допировании

Rotation of magnetic field from “out of plane” to “in-plane”:
Falling mode is conserved in pure sample and smeared in the doped sample .

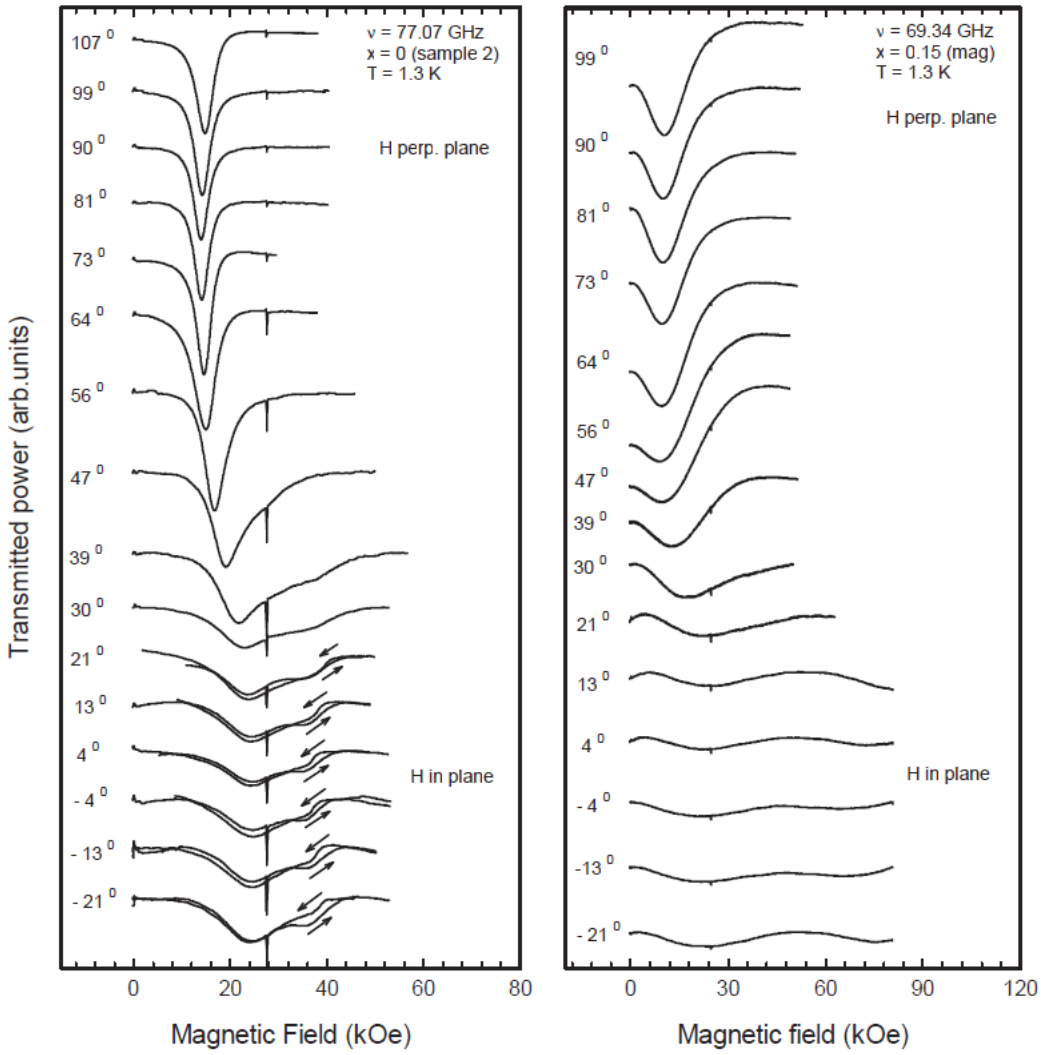

Pure

Doped

Triangular Antiferromagnet with Nonmagnetic Impurities

V. S. Maryasin and M. E. Zhitomirsky
Service de Physique Statistique, Magnétisme et Supraconductivité,

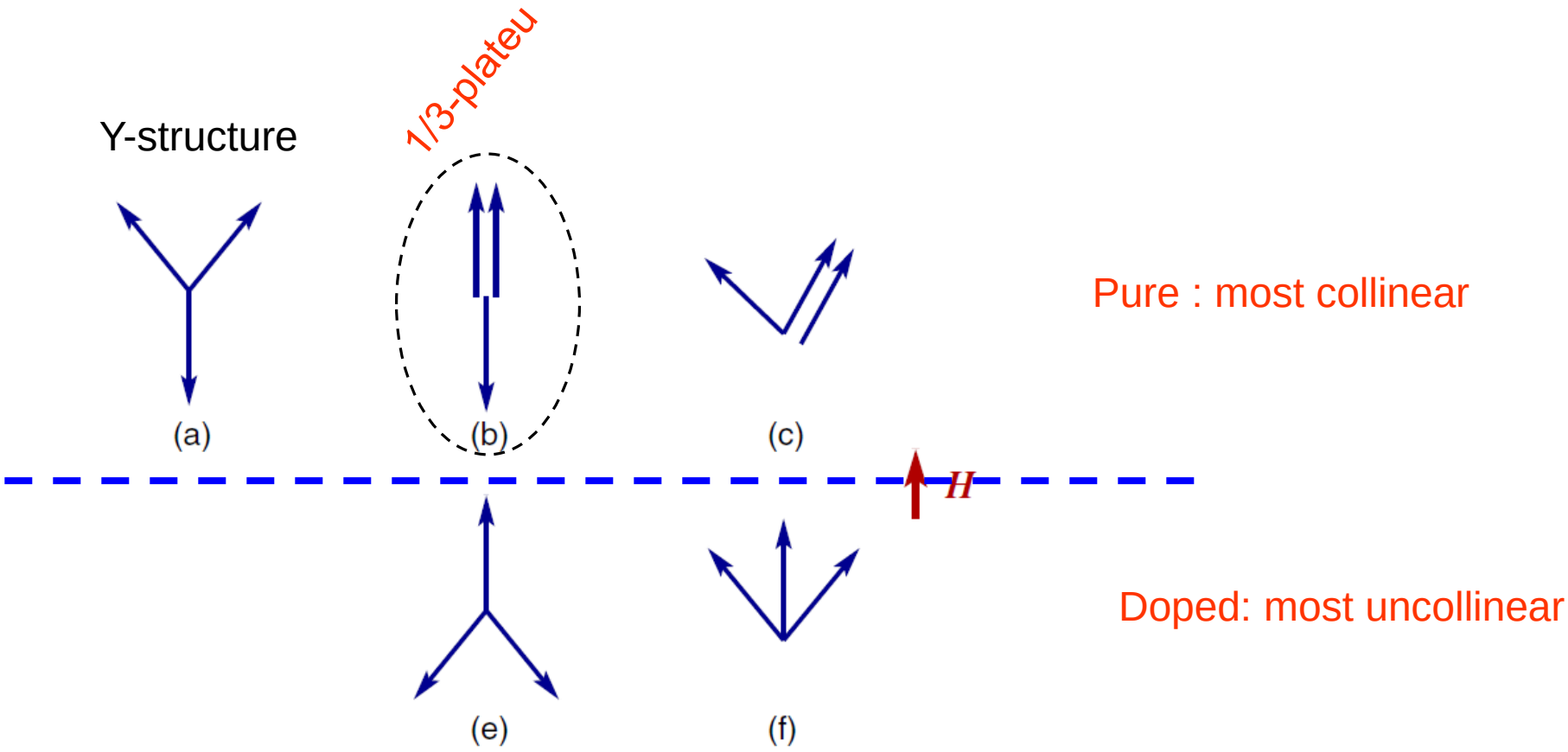

Выводы:

Кривые намагничивания подтверждают выключение флуктуационного механизма отбора основного состояния при введении примесей

Спектры ЭСР подтверждают кардинальную смену основного состояния и находятся в соответствии со сменой Y структуры на анти-Y структуру.

Резкий отклик на немагнитное допирование показывает, что флуктуации действительно важны для отбора основного состояния в треугольном антиферромагнетике

Спасибо за внимание

СПЕКТРИНА 2018

ПИЯФ Гатчина 19 апреля

Triangular antiferromagnets with “easy plane” anisotropy have similar phase diagram for in-plane magnetic field.

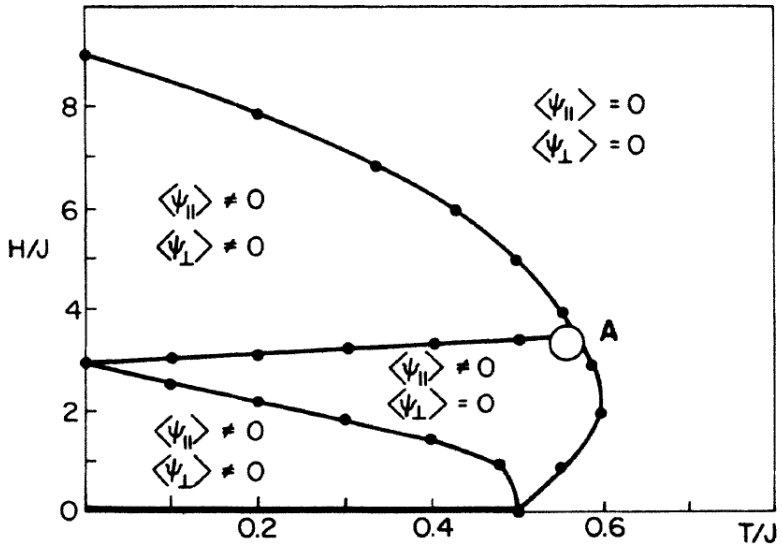

FIG. 15. Phase diagram for AFP model on a triangular lattice. Four phases can be identified and are labeled by the behavior of the order parameters $\psi_{||}$ and $\psi_{\perp}$. The manner in which the three phase boundaries merge at A is not determined precisely in this work.

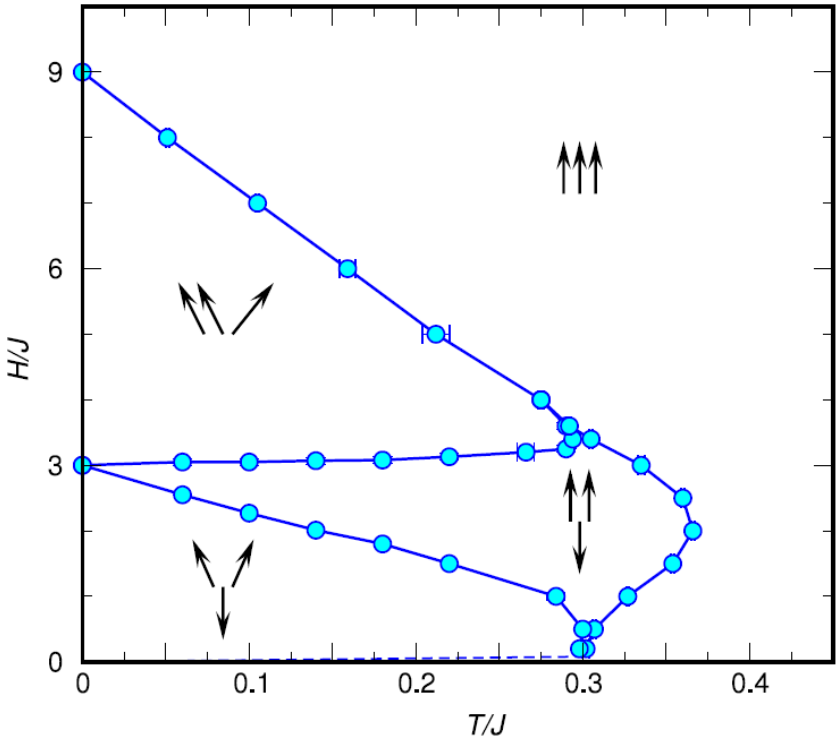

Figure 3. Magnetic field phase diagram of the Heisenberg triangular-lattice antiferromagnet. Transition points determined by the Monte Carlo simulations are shown by circles. Solid lines are guides for the eye. Dashed line indicates the position of additional low-field transitions.

XY-model, MC simulations, *Lee et al PRB 1986*

Heisenberg model, MC simulations
M V Gvozdikova, P-EMelchy
and M E Zhitomirsky JPCM2011

ESR modes in a triangular antiferromagnet with easy-plane anisotropy, in-plane magnetic field

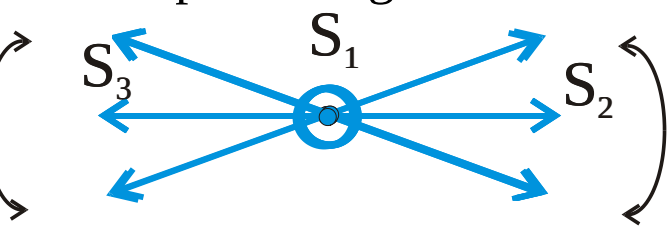

S_1 does not leave the plane

α-mode

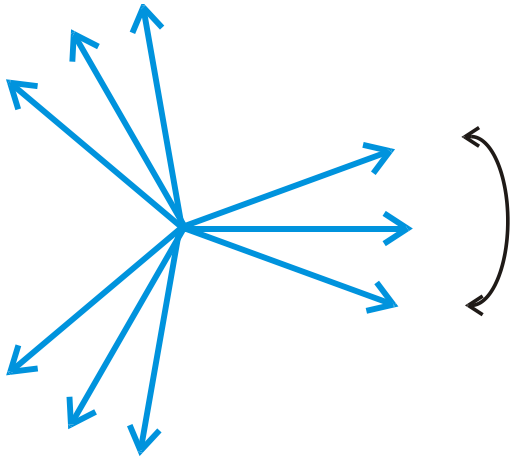

in-plane spin oscillations (Goldstone mode),

β-mode

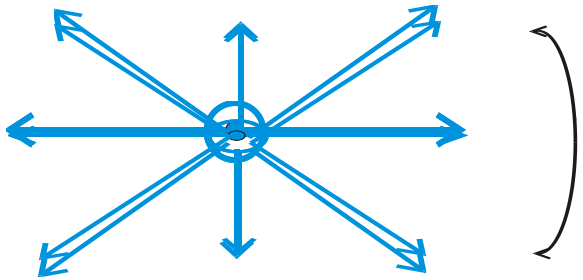

out-of-plane oscillations of all 3 sublattices.

γ-mode.

ESR spectrum of pure and ***doped*** $RbFe(MoO_4)_2$

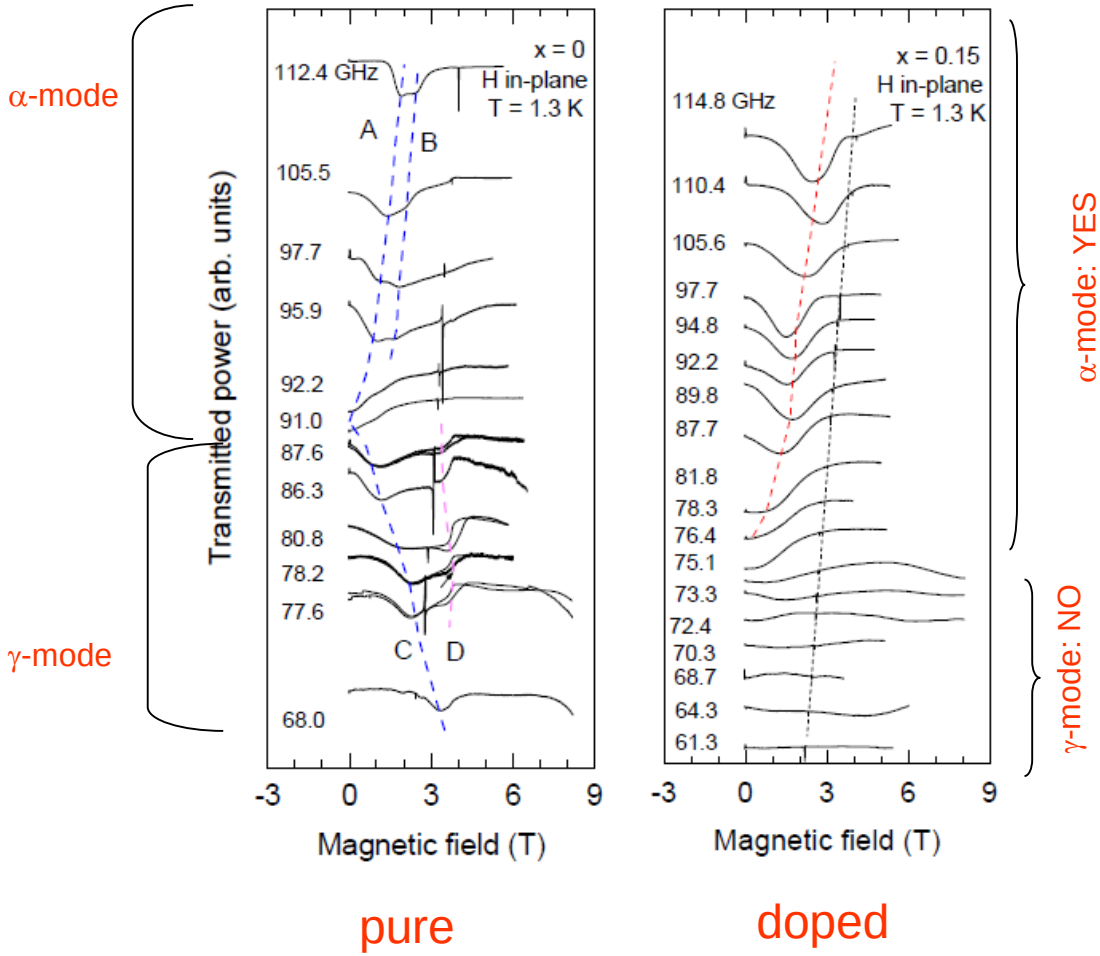

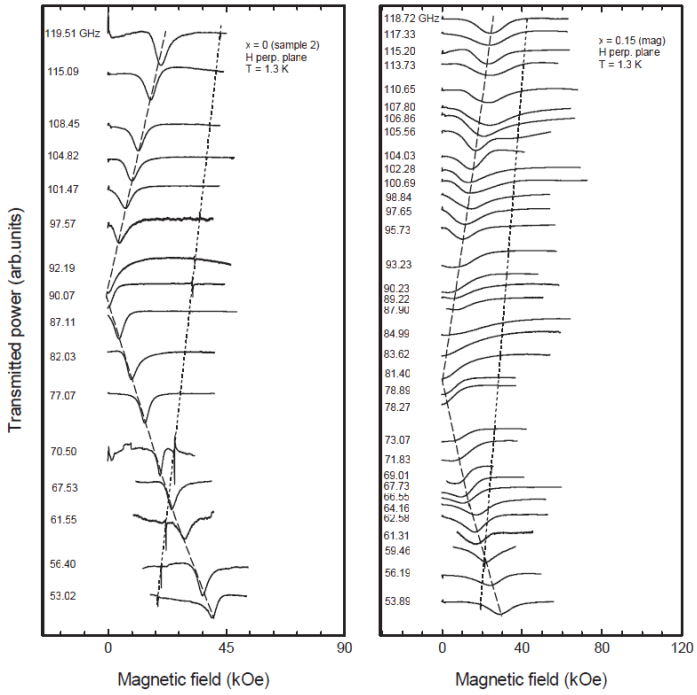

<u>in-plane magnetic field</u> :
Y-structure is not adequate for doped sample

<u>out-of-plane magnetic field :</u>
Both rising and falling modes are present. For this orientation there is no degeneracy and no "order-by-disorder" because of easy-plane anisotropy.

Rotation of magnetic field from “out of plane” to “in-plane”:
Falling mode is conserved in pure sample and smeared in the doped sample .

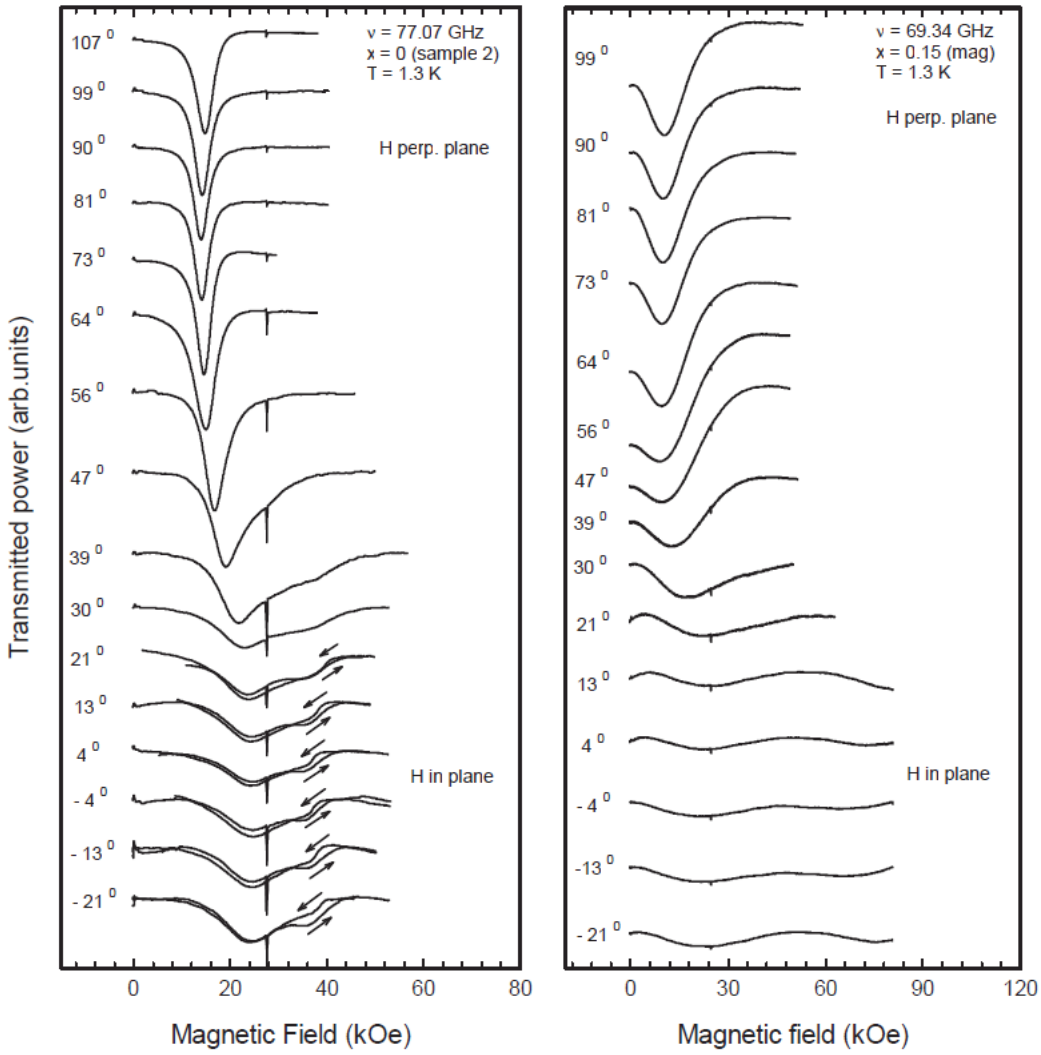

Pure

Doped

Outline of ESR spectra for pure and doped samples

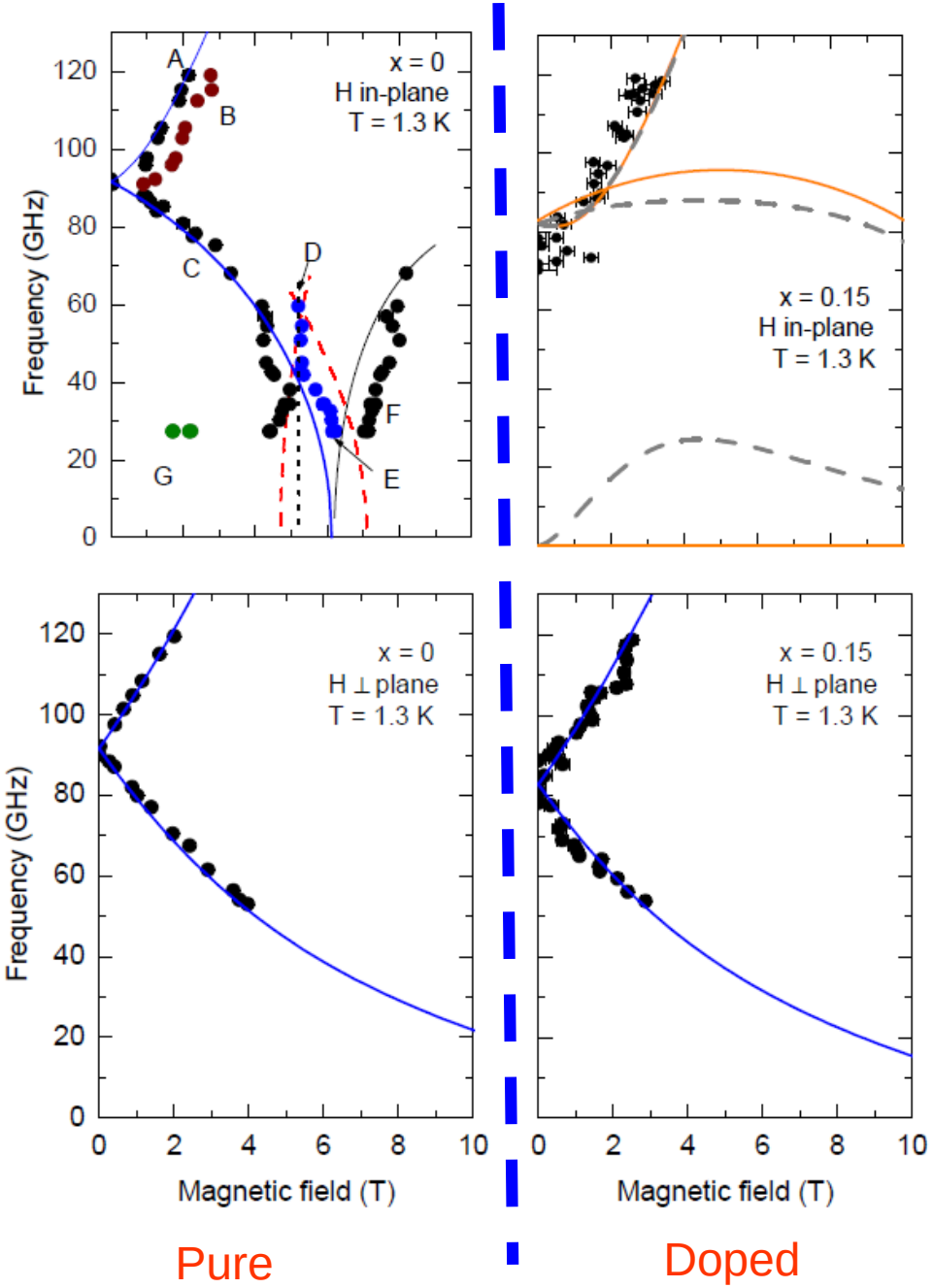

Theory for Y-structure

Theory for anti-Y-structure
With two values of
biquadratic exchange

Theory for umbrella-structure

Change of the ESR spectrum corresponds to "Y"- "anti Y" transition due to doping